UvA-DARE (Digital Academic Repository)

Decreased Hypothalamic Glucagon-Like Peptide-1 Receptor Expression in Type 2 Diabetes Patients

ten Kulve, J.S.; van Bloemendaal, L.; Balesar, R.; IJzerman, R.G.; Swaab, D.F.; Diamant, M.; la Fleur, S.E.; Alkemade, A.

Citation for published version (APA):

ten Kulve, J. S., van Bloemendaal, L., Balesar, R., IJzerman, R. G., Swaab, D. F., Diamant, M., la Fleur, S. E., & Alkemade, A. (2016). Decreased Hypothalamic Glucagon-Like Peptide-1 Receptor Expression in Type 2 Diabetes Patients. *Journal of clinical endocrinology and metabolism*, *101*(5), 2122-2129. https://doi.org/10.1210/jc.2015-3291

Decreased Hypothalamic Glucagon-Like Peptide-1 Receptor Expression in Type 2 Diabetes Patients

Jennifer S. ten Kulve,* Liselotte van Bloemendaal,* Rawien Balesar, Richard G. IJzerman, Dick F. Swaab, Michaela Diamant,† Susanne E. la Fleur,‡ and Anneke Alkemade‡

Diabetes Center and Department of Internal Medicine (J.S.t.K., L.v.B., R.G.I., M.D.), VU University Medical Center, 1007 MB Amsterdam, The Netherlands; Amsterdam Brain and Cognition Center (R.B., A.A.) and Department of Endocrinology and Metabolism (S.E.l.F.), Academic Medical Center, University of Amsterdam, 1100 DE Amsterdam, The Netherlands; and Department of Neuropsychiatric Disorders (D.F.S.), Netherlands Institute for Neuroscience, An Institute of the Royal Netherlands Academy of Arts and Sciences, 1105 BA Amsterdam, The Netherlands

Context: Glucagon-like peptide-1 (GLP-1) and GLP-1 receptor agonist treatment in type 2 diabetes (T2DM) reduce blood glucose and food intake. It has been suggested that these effects are partly mediated through central GLP-1 receptors (GLP-1Rs). The rodent and nonhuman primate hypothalamus show clear GLP-1R expression. However, a detailed description of GLP-1R expression in the human hypothalamus is lacking, and it is unknown whether this expression is altered in T2DM patients.

Objective: The objective of the study was to investigate the GLP-1R distribution in the human postmortem hypothalamus and to determine whether hypothalamic GLP-1R expression is altered in T2DM patients.

Design: We investigated the distribution of GLP-1R expression throughout the human hypothalamus by means of in situ hybridization. We also performed quantifications of GLP-1R mRNA expression in two hypothalamic nuclei (ie, the paraventricular nucleus [PVN] and infundibular nucleus [IFN]), comparing patients with T2DM and control subjects.

Results: We found that GLP-1R mRNA was expressed in a number of hypothalamic nuclei including the PVN and the IFN, both involved in the regulation of energy metabolism. We observed sporadic colocalization of the GLP-1R in the IFN with the orgexigenic neuropeptide Y, agouti-related peptide, or proopiomelanocortin transcripts. Comparison of GLP-1R mRNA in the PVN and IFN between T2DM patients and control subjects revealed a decreased expression in T2DM patients.

Conclusions: Our studies show that GLP-1R is widely expressed throughout the human hypothalamus. The decreased expression of GLP-1R in the PVN and IFN of T2DM patients may be related to the dysregulation of feeding behavior and glucose homeostasis in T2DM. (*J Clin Endocrinol Metab* **101: 2122–2129, 2016**)

Glucagon-like peptide-1 receptor agonists (GLP-1RAs) lower blood glucose via stimulating insulin secretion and inhibiting glucagon release and are therefore used for treatment of type 2 diabetes mellitus (T2DM) (1). Interestingly, in addition to the glucose lowering properties, T2DM patients taking GLP-1RAs report reduced appetite and food intake contributing to weight loss (2–4).

GLP-1RAs are derivatives of the naturally occurring peptide hormone glucagon-like peptide-1 (GLP-1), which is secreted from intestinal enteroendocrine L cells in response to nutrient ingestion. A large number of studies in humans investigated peripheral effects of GLP-1 and GLP-1RAs on pancreatic islet cells, liver, and stomach (5, 6). However, from rodent and nonhuman primate studies, it is clear that GLP-1 is also centrally produced in the nucleus of the solitary tract in the brainstem. These GLP-1-producing neurons show projections throughout the brain including the hypothalamus, an area of particular importance for the regulation of both feeding behavior and glucose metabolism (7, 8). Within the rodent hypothalamus, GLP-1R expression has been demonstrated using in situ hybridization in a number of nuclei that play a role in the regulation of energy metabolism. These areas include the infundibular nucleus (IFN) (or arcuate nucleus [ARC] as it is called in rodents) and the paraventricular nucleus (PVN) (9). This observation suggests that, in addition to GLP-1 effects on metabolism and feeding behavior via receptors in peripheral organs, there may be central effects of this peptide. Indeed, animal experiments support central effects as well (7, 9–11). GLP-1 administration in the ARC of rats improves glucose homeostasis by regulating hepatic glucose production (12) and GLP-1 administration into the PVN of rats reduces food intake (13).

Less is known about the central effects of GLP-1 and the expression of the GLP-1R in the human brain. Given the increasing interest and use of GLP-1-based therapies and the emerging evidence that the brain is involved in glucose control, information on GLP-1R expression in the human hypothalamus of control subjects and patients suffering from T2DM is also of clinical interest. GLP-1 binding and in situ hybridization of GLP-1R mRNA have been reported in the human hypothalamus (14). This study did not, however, provide a detailed description of the distribution within the hypothalamus. In the present study, we therefore investigated the distribution of GLP-1R mRNA in the human postmortem hypothalamus using in situ hybridization. In view of the role of the PVN and ARC in the regulation of glucose metabolism and feeding behavior in rodents, we performed quantifications of GLP-1R mRNA expression in the PVN and IFN, comparing patients with T2DM and control subjects. We hypothesized that the expression of the GLP-1R in these hypothalamic nuclei is altered in T2DM patients compared with control subjects. GLP-1R mRNA expressing cells of the IFN were further characterized using double labeling with the orexigenic neuropeptide Y (NPY) and agouti-related peptide (AgRP) as well as the anorexigenic proopiomelanocortin (POMC).

Materials and Methods

Subjects

In experiment 1 we studied the distribution of the GLP-1R using systematic sampling covering the entire rostrocaudal axis of the hypothalamus in human postmortem tissue. We analyzed six subjects (four male) without clinical neurological or neuropsychiatric diseases or T2DM, ranging in age between 60 and 81 years. Clinicopathological data of subjects in experiment 1 are presented in Table 1. In experiment 2 we quantified the expression of the GLP-1R in the PVN and IFN of the hypothalamus. We studied eight subjects with T2DM and eight control subjects, without neurological or neuropsychiatric disorders ranging in age between 65 and 89 years (Table 1). The diagnosis of T2DM and the used medication were available from the clinical records and have in part been reported previously (15). All brain material was obtained from The Netherlands Brain Bank (TNBB) at The Netherlands Institute for Neuroscience in accordance with the formal permissions for brain autopsy and for the use of human brain material and for clinical information for research purposes. Registration as a donor for TNBB is voluntary, without any payment or undue incentives. All material and data collected by TNBB are obtained on the basis of written informed consent.

Histology

Brains were dissected at autopsy and the (hemi-) hypothalamus was fixed in 4% phosphate-buffered formalin at room temperature for 4–15 weeks (Table 1). After dehydration in graded ethanol series, tissues were cleared in toluene and embedded in paraffin. Serial coronal sections (6 μm) were cut from the level of the lamina terminalis to the caudal border of the mammillary bodies. For anatomical orientation, every 100th section was collected and mounted on Superfrost Plus slides (Menzel Glaser), dried for at least 2 days at 37°C, and stained with thionine. In experiment 1 (distribution study), GLP-1R in situ hybridization (ISH) was performed using systematic sampling (600 μm intervals) over the entire rostrocaudal axis of the hypothalamus. In experiment 2 (quantification), we used thionine staining for anatomical orientation, and GLP-1R ISH was performed on a central cross-section of the IFN and PVN.

Locked nucleic acid probe

A locked nucleic acid (LNA) probe (LNA-2′-O-methyl-RNA) specific for the human GLP-1R mRNA sequence was designed (16). This technique has been applied successfully to postmortem human brain tissue (17). We applied an antisense probe 3′-GTC-CTTGAGGTTGTACTTG-5′ complementary to bases 953–972 of the human GLP-1R (GenBank NM_002062.3). A scrambled sequence was used as a negative control. Probes were FAM tagged at the 5′ end and custom ordered (Ribotask, Langeskov).

Table 1. Clinicopathological Data

Subject	Sex	Ag, y	PMD, h	Fix, d	Group	Cause of Death, Clinical Diagnoses
Distribution study						
98-161	F	60	8	87	CO	Pneumonia, ovarian ca. (Mx)
08-052	F	62	8	73	CO	RI, renal cell ca. (Mx)
98-030	M	63	2:30	108	CO	RI, squamous cell ca oropharynx (Mx)
93-061	M	70	5	28	CO	Pneumonia, RI, bronchus ca., hepatomegalia, atherosclerosis
00-090	M	70	7:30	34	CO	RI, bladder ca. (Mx)
10-008	M	81	4:50	53	CO	AP, hypercholesterolemia, adenocarcinoma, artheritis
n/med	M/F 4/2	66.5	6.15	63		
Quantification study						
98-198	M	65	33	76	CO	MI, anemia, COPD, bronchial ca.
98-122	M	66	41	49	CO	RI, adenoca. (Mx)
99-101	M	69	19	41	CO	RI, infarction distal brainstem, alcohol abuse, HT
00-090	M	70	7:30	34	CO	RI, bladder ca. (Mx)
98-095[a]	F	75	ND	63	CO	RI, pneumonia, COPD, MI, mycosis, atrial fibrillation
01-005	F	76	20	36	CO	RI, NHL, HT, basal cell ca.
00-007	M	85	15	35	CO	MI, bladder ca.
99-046[a]	F	89	5	36	CO	MI, heart failure, mitral valve insufficiency
n/med	5/3	72.5	19	38.5		
97-060	M	65	59:30	36	T2DM	MI, DC, T2DM (tolbutamide, metformin)
03-054	M	67	4:50	50	T2DM	Cardiogenic shock, MOF, T2DM (insulin metformin), COPD
02-087[b]	M	71	7:30	38	T2DM	RI, MOF, T2DM (gliclazide)
97-088	F	78	4	33	T2DM	Pneumonia, CVA, T2DM (gliclazide)
82-019	M	83	56	35	T2DM	MI, CVA, pneumonia, osteosynth. collum fracture, T2DM (metformin, tolbutamide)
98-056	F	83	5	41	T2DM	RI, colon ca., T2DM (no data on medication), cataract, arthrosis
98-055[b]	M	85	21:30	31	T2DM	DC, MI, T2DM (glibenclamide)
95-016	F	86	13:50	30	T2DM	DC, AP, nephropathy, retinopathy, T2DM (tolbutamide)
n/med	M/F 5/3	80.5	10:30	35.5		

Abbreviations: AP, angina pectoris; ca., carcinoma; CO, controls; COPD, chronic obstructive pulmonary disease; CVA, cardiovascular accident; DC, decompensatio cordis; F, female; Fix, fixation duration; HT, hypertension; M, male; MI, myocardial infarction; med, median; MOF, multiorgan failure; Mx, metastasized; NA, not applicable; NHL, non-Hodgkin lymphoma; PMD, postmortem delay; RI, respiratory insufficiency.

[a] Excluded for IFN analysis due to tissue damage.

[b] Excluded for all analyses due to tissue damage.

Specificity of the probe was further assessed by testing of a concentration gradient ranging from 1 pM to 25 nM.

In situ hybridization

Sections were deparaffinized in xylene and rehydrated through a graded series of ethanol followed by rinsing in PBS. Sections were equilibrated for 2 minutes in 0.01 M sodium citrate buffer (pH 6.0) and microwaved at 800 W for 2×5 minutes. After cooling and rinsing in PBS, sections were deproteinated with 0.2 N HCL for 20 minutes followed by 15 minutes of proteinase K digestion at 2 μg/mL at 37°C. Reaction was stopped in a glycin buffer. Delipidation was performed using 0.1% Triton X-100 for 10 minutes, which was followed by a 30–60 minutes of prehybridization in a humidified chamber at 55°C in hybridization buffer (not containing probe) with final concentrations of 50% (vol/vol) deionized formamide, 600 mM NaCl, 10 mM HEPES (pH 7.5), $5\times$ Denhardt's, 1 mM EDTA, and 200 μg/mL denatured herring sperm DNA (Invitrogen Life Technologies; catalog number 15634–017). For hybridization, the antisense GLP-1R probe was diluted in hybridization buffer to a final concentration of 3 nM, denatured at 95°C for 5–10 minutes, and cooled on ice. Sections were covered and hybridized overnight at 55°C and subsequently washed for 5 minutes each in $2\times$ standard sodium citrate buffer (SSC; 0.3 M NaCl, 0.03 M trisodium citrate dihydrate), $0.5\times$ SSC, and $0.2\times$ SSC at 55°C and for 5

minutes in Tris-buffered saline (TBS; 0.05 M Tris-HCl, pH 7.6; 0.15 M NaCl) at room temperature.

Next, sections were incubated with anti-fluorescein-alkaline phosphatase Fab fragments (Roche Life Science; catalog number 11426338910) at 1:3000 in Supermix (0.25% [wt/vol] gelatin and 0.5% [vol/vol] Triton X-100 in TBS) for 3 hours at room temperature. Slides were washed 3×5 minutes in TBS, rinsed in buffer 2 (100 mM Tris-HCl, pH 9.5; 100 mM NaCl; and 5 mM $MgCl_2$), followed by color development using nitroblue tetrazolium chloride (NBT)-5-bromo-4-chloro-3-indolyl phosphate (BCIP) solution (buffer 2 containing 0.34 mg/mL NBT [Roche Life Science; catalog number 1585029001], 0.18 mg/mL BCIP [Roche Life Sciences; catalog number 11585002001]) and 0.24 mg/mL levamisole (Sigma-Aldrich; catalog number L9756) for 20–30 minutes under dark conditions. Sections were then washed in distilled water, rinsed in methanol (Sigma-Aldrich; catalog number 34860) for 5 minutes, and rinsed again in distilled water. Finally, slides were coverslipped using Kaiser's glycerine (Merck Millipore; catalog number 109242) and stored at 4°C for until further processing.

Distribution

In experiment 1 staining intensity was scored by visual inspection under a microscope in a semiquantitative fashion: − (no staining), +/− (few positive cells showing light staining inten-

sity), + (most cells are positive and cells show a moderate to strong signal), and ++ (most cells are positive and staining intensity is high). Every 100th 6-μm section was scored systematically over the entire rostrocaudal axis. Two researchers scored staining intensities (J.S.t.K. and L.v.B.).

Quantitative analysis

All sections were hybridized within the same experiment. Sections were digitally scanned and GLP-1R staining was quantified using a thresholding procedure in ImageJ (V1.49n, ImageJ.net). The threshold settings were determined experimentally and set to 116 for all further analyses. Multiplication of the mean OD and the fraction of the outlined surface covered by the mask resulted in a quantitative value expressed in arbitrary units (a.u.).

Double labeling

To further characterize GLP-1R-expressing neurons in the IFN, colocalization studies were performed for POMC, AgRP, and NPY. Paraffin IFN sections were stained from four control subjects, one male and three females, ranging in age from 77 to 100 years. Antibody staining was performed before GLP-1R mRNA detection. The following antibodies were applied: anti-AgRP at 1:750 (catalog number H-003–053; Phoenix Pharmaceuticals), anti-NPY at 1:500 (Niepke, bleeding 091 188; The Netherlands Institute for Neuroscience) (18), and anti-αMSH as a marker for POMC neurons at 1:2000 (NHI4372, bleeding 230 475; The Netherlands Institute for Neuroscience) (19, 20). Antibody specificity has been described previously for all antibodies including preadsorption studies with the homologous peptide and cross-adsorption with independent peptides (18, 19). Double-labeling experiments and subsequent analyses using spectral analyses have been described previously, with minor adaptations (17, 21). For AgRP and NPY, the peroxidase-antiperoxidase detection was used and the avidin biotin complex method was used for POMC. Staining was visualized with 0.5 mg/mL diaminobenzidine. The ISH procedure was performed as describe above. The GLP-1R LNA probe was applied at concentrations of 20–40 nM. ISH signal was developed using NBT-BCIP.

We used the Nuance multispectral imaging system (NuanceFX camera [PerkinElmer] connected to a Zeiss Axioskop microscope with Plan-NEOFLUAR Zeiss objectives; Carl Zeiss GmbH) for the spectral analyses. For each chromogen, a spectral library was defined using single-stained sections. Colocalization was evaluated by unmixing spectral libraries on double-stained sections. Pseudofluorescence was used for visualization purposes.

Statistical analysis

Analyses of quantitative data were performed with the Statistical Package for the Social Sciences version 20. We did not assume normal distribution of the data and performed conservative nonparametric statistical analyses. Group differences were analyzed using a Mann-Whitney U test. $P < .05$ was considered statistically significant.

Results

Specificity

ISH specificity was supported by the absence of signal using the scrambled sequence (Supplemental Figure 1).

Specificity was additionally supported by the decrease in signal observed with increased dilution of the probe. Specificity of the antibodies used for colocalization studies was published previously (18, 20).
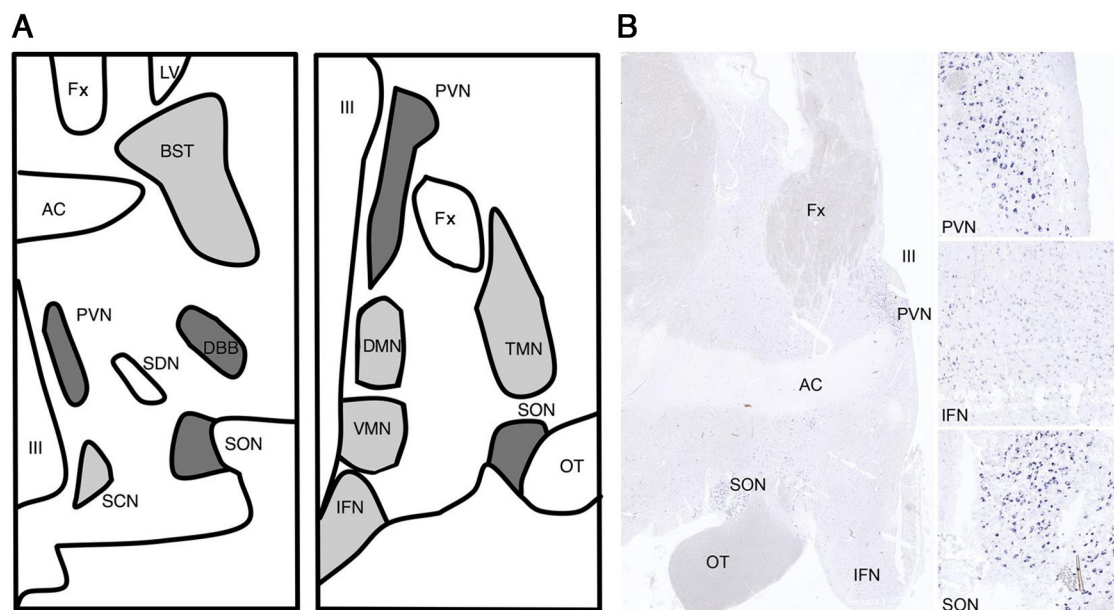
Distribution of GLP-1R mRNA

GLP-1R mRNA-positive cells were present in a number of hypothalamic nuclei (Figure 1). The distribution pattern of GLP-1R mRNA was in general agreement between the six subjects, although a strong interindividual variation was observed in staining intensity (Table 2). Intense ISH signal was present in the PVN, supraoptic nucleus (SON), diagonal band of Broca (DBB), ventromedial nucleus (VMN), dorsomedial nucleus (DMN), and nucleus basalis of Meynert (NBM). Staining was also present in the IFN, suprachiasmatic nucleus (SCN), lateral hypothalamic area, bed nucleus striaterminalis (BST), preoptic area, tuberomammillary nucleus (TMN), and mammillary body.

Colocalization studies revealed sporadic colocalization in the IFN between GLP-1R mRNA and NPY, AgRP, and POMC (Figure 2).

Comparison of GLP-1R mRNA expression between T2DM and control subjects

Eight subjects with T2DM and eight control subjects were compared for GLP-1R expression in the PVN and IFN. Tissue damage was observed in the PVN in two T2DM patients, who were deemed unsuitable for further analyses (number 02–087 and number 98–055). We decided not to retest these two subjects in view of the significant interassay variation we observed during the piloting phase. Therefore, subjects were not closely matched and a conservative Mann-Whitney U test was used for statistical analyses. GLP-1R expression in the PVN was lower in T2DM patients compared with control subjects ($U = 4.0$; $P = .008$) (Figure 3A). The IFN of two control subjects was damaged and these samples were deemed unsuitable for further analyses (number 98–095 and number 99–046). GLP-1R expression in the IFN was also lower in T2DM patients compared with control subjects ($U = 0.0$; $P = .002$) (Figure 4A). Examples of the differences in GLP-1R staining in PVN and IFN between T2DM and control subjects are illustrated in Figures 3B and 4B. Age, sex, postmortem delay, and fixation duration were not significantly different between groups ($P > .2$). Data on body mass index (BMI) was available in two control subjects (24 and 32 kg/m^2) and in four T2DM patients (range 20–35 kg/m^2) and could therefore not be analyzed in a reliable fashion.

Figure 1. Distribution of the GLP-1R in coronal sections of human hypothalamus. A, Schematic illustration of distribution of GLP-1R in coronal sections of human hypothalamus. Dark gray coloring indicates areas showing intense staining for GLP-1R represents staining for GLP-1R, and light gray indicate less intense staining. B, Photomicrographs showing GLP-1R staining throughout the hypothalamus including detailed photomicrographs of PVN, IFN, and SON. AC, anterior commissure; Fx, fornix; III, third ventricle; LV, lateral ventricle; OT, optic tract; SDN, sexually dimorphic nucleus.

Discussion

We show that GLP-1R mRNA is expressed throughout the human hypothalamus, comparable with what has been reported in rodents and nonhuman primates (9, 10), with most pronounced expression in the PVN, SON, DBB, and NBM. Additional staining was observed in other nuclei involved in the regulation of energy metabolism such as the VMN, DMN, IFN, and SCN. Most importantly, we found a decreased expression of the GLP-1R in both the PVN and IFN of T2DM patients. A minority of GLP-1R mRNA-expressing neurons showed coexpression of NPY, AgRP, and POMC. Future studies will be needed to further characterize these neurons.

Some differences with the localization of GLP-1R in rodents and nonhuman primates should be noted. Expression of GLP-1R in the VMN has not been reported in rodents, using ISH, or in nonhuman primates, using both

ISH and immunohistochemistry with a GLP-1R monoclonal antibody (9, 10). In the present study, we did observe a clear expression of GLP-1R mRNA in the human VMN. Our observation is in line with an earlier report on GLP-1R expression in the human brain using ISH (14). Whether this observation represents an interspecies difference remains unclear.

From rodent studies it is clear that GLP-1 affects energy metabolism by acting on the ARC (IFN) and the PVN. Chemical ablation of the ARC in rats prevents the inhibitory action of GLP-1 on feeding (22); GLP-1 infusion into the ARC lowers hepatic glucose production, thereby reducing blood glucose (12); and direct injection of GLP-1 in the PVN of rats leads to decreased food intake (13). It is possible that decreased GLP-1R expression in the IFN and PVN in T2DM patients contributes to dysregulation of glucose homeostasis and feeding behavior as reported in

Table 2.   Distribution of GLP-1R mRNA in the human hypothalamus

Subject	PVN	IFN/ME	VMN/DMN	SON	SCN	LHA/PFo	DBB	NBM	BST	POA	TMN	MB
98-161	+	+	+	+	−	−	++	+	+	−	+	+/−
08-052	+	−	+	++	+	+	++	+	+	+	++	+
98-030	++	+	+	++	+	−	++	++	+	++	++	−
93-061	++	+	++	++	+	−	++	++	+	+	+	++
00-090	++	++	++	++	+	+	++	++	+	+	+	++
10-008	++		++	++	−	+	+	++	+	−	++	−

Abbreviations: LHA, lateral hypothalamic area; PFo, periformical nucleus; ME, median eminence; POA, preoptic area; MB, mammillary body; −, no staining; +/−, few positive cells showing light staining intensity; +, the majority of cells are positive and cells show a moderate to strong signal; ++, the majority of cells are positive and staining intensity is high.
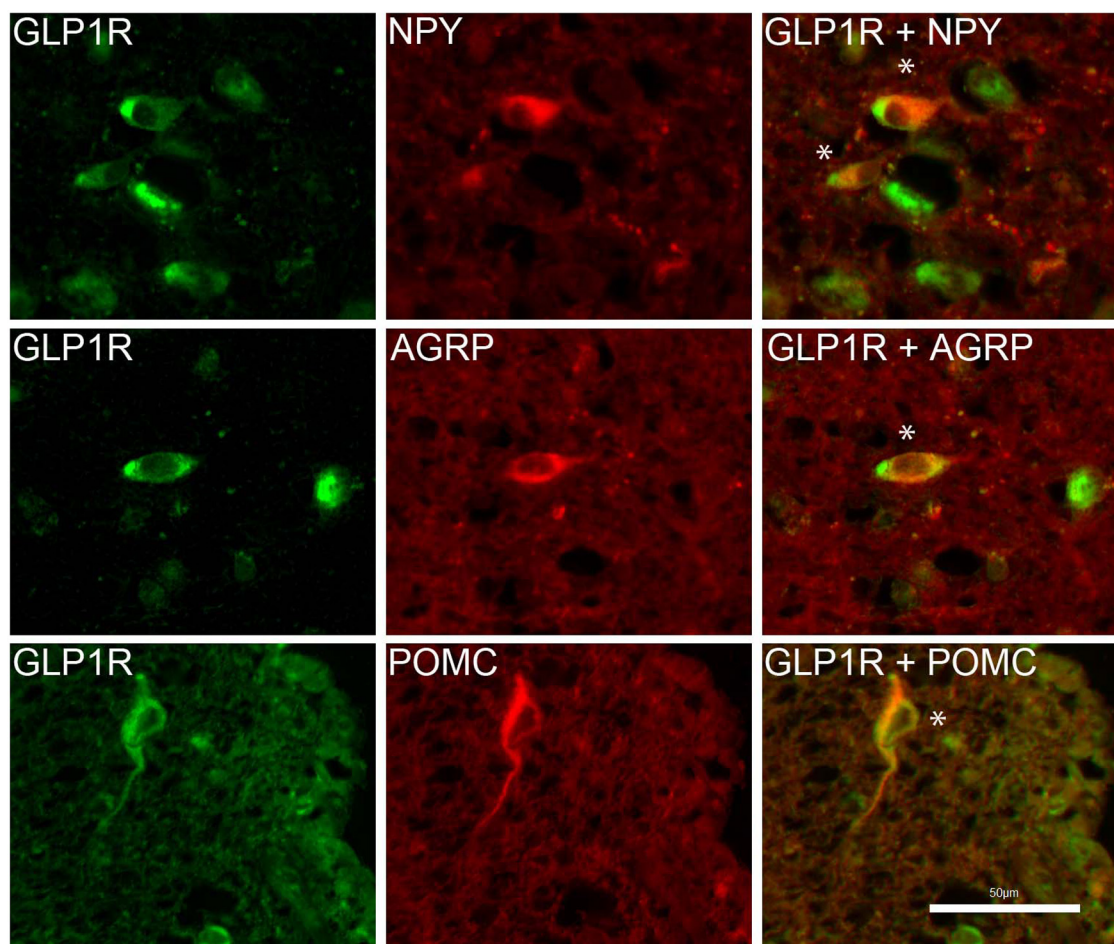
Figure 2. Colocalization of GLP-1R expression and NPY, AgRP, and POMC in the IFN. Photomicrographs showing GLP-1R staining (in green) combined with, respectively, NPY, AgRP, and POMC (in red). Scale bar, 50 μm.

T2DM. Alternatively, in rats a hyperglycemic state decreases GLP-1R expression in pancreatic islets (23), which could indicate that the decreased GLP-1R expression could be a consequence of a hyperglycemic state.

We observed sporadic colocalization of GLP-1R expression and NPY/AgRP and POMC. Although specula-

tive, the expression of GLP-1Rs on neurons expressing NPY/AgRP and POMC may indicate that GLP-1 affects energy metabolism via actions on these hypothalamic neurons. We have shown in our previous studies that alterations in NPY and AgRP expression were related to BMI, whereas expression of the POMC derived αMSH was re-
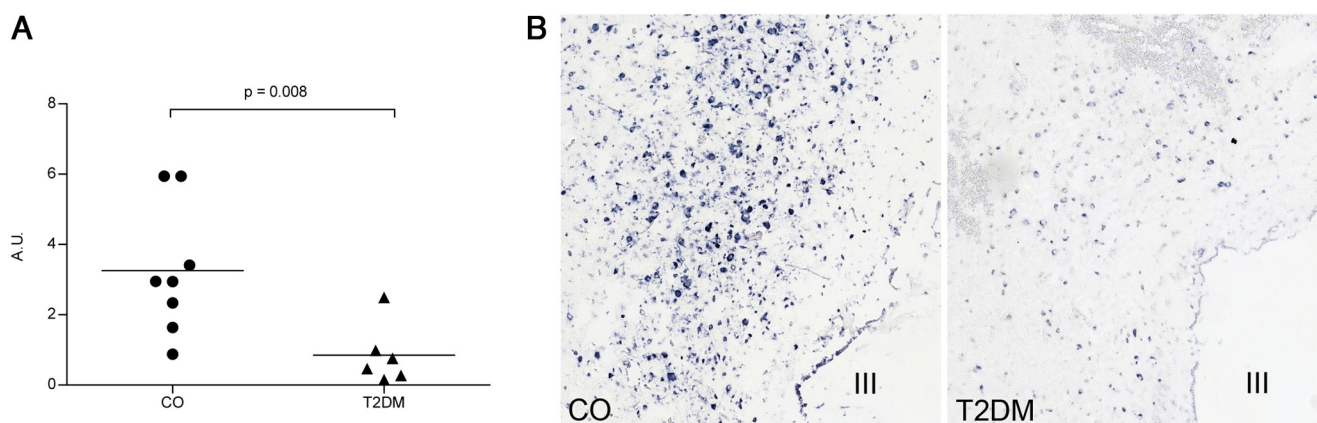
Figure 3. GLP-1R mRNA expression in the PVN in controls subjects compared with T2DM patients. A, GLP-1R mRNA expression in control subjects compared with T2DM patients in the PVN. Two T2DM subjects (number 02–087 and number 98–055) were not included in the analysis due to tissue damage. B, Representative images of GLP-1R staining in the PVN of a control subject and in a T2DM patient. CO, control subjects; III, third ventricle.
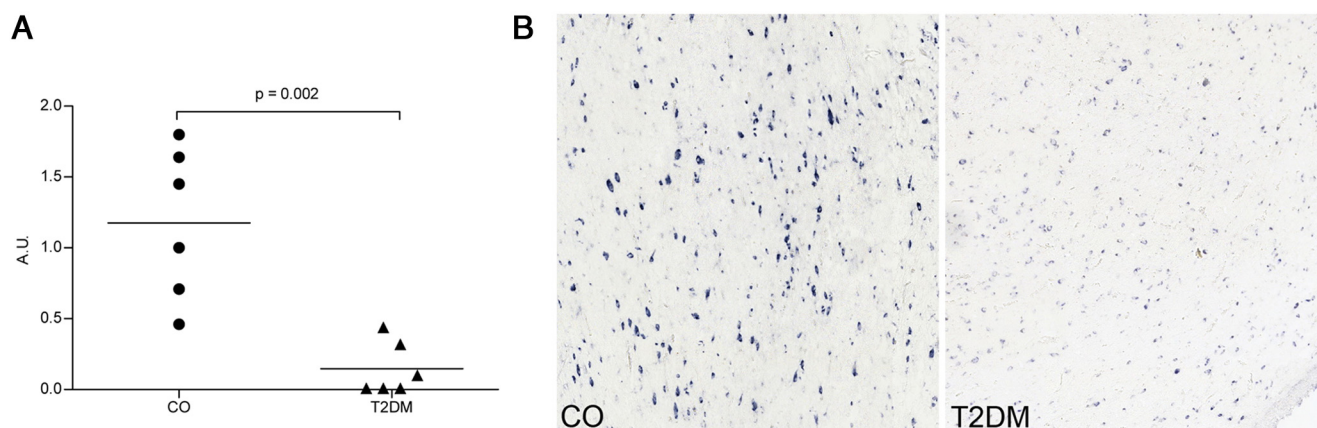
Figure 4. GLP-1R mRNA expression in the IFN in controls subjects compared with T2DM patients. A, GLP-1R mRNA expression in control subjects compared with T2DM patients in the IFN. Two control subjects (number 98–095 and number 99–046) were not included in the analysis due to tissue damage. B, Representative images of GLP-1R staining in the IFN of a control subject and in a T2DM patient. CO, control subjects; III, third ventricle.

lated to T2DM (15). Interestingly, it has been shown in rats that GLP-1 directly stimulates POMC neurons and that the GLP-1R on POMC neurons in the ARC plays a role in mediating the anorectic effects of GLP-1RA (24–26). Furthermore, fasting GLP-1 levels were shown to be positively associated with body fat mass (27). In the present study, we were unable to relate our data to BMI because these data were available in only a small number of the subjects included. Additionally, colocalization was only sporadic, and therefore, functional implications may be limited.

The use of human postmortem tissues has a number of inherent limitations. The availability of well-documented material is limited, resulting in a relatively low number of observations in subjects with advanced age. We investigated available clinical records, but data on BMI and biochemical characteristics at the end stage of life were often not reported. Despite a relatively low number of observations, we found significant differences in GLP-1R expression. Whether age affects GLP-1R expression is currently unknown.

All T2DM patients in our study were treated with glucose-lowering agents, ie, metformin and/or a sulfonylurea derivative. We cannot exclude that these compounds may have influenced GLP-1R expression. However, it was shown that metformin increases GLP-1R mRNA expression in murine islet cells (28). Because we observed a decrease in GLP-1R expression in T2DM patients, potential effects of metformin may have led to an underestimation of the observed effect. To our knowledge, no effects of sulfonylurea derivatives on GLP-1R expression have been reported in literature.

Using postmortem studies, it is impossible to determine causality. Additionally, it is unknown whether GLP-1R expression is altered throughout the brain or that changes are limited to the hypothalamus. It remains to be clarified whether T2DM patients have altered sensitivity to GLP-1RA, which are used for the treatment of obesity and T2DM. These questions provide clear future directions for further research.

To conclude, we describe the systematically determined distribution of the GLP-1R in the human hypothalamus. Our main finding was a decreased expression of the GLP-1R in T2DM patients in the IFN and PVN. This decreased expression of the GLP-1R may be related to the dysregulation of feeding behavior and glucose homeostasis in T2DM patients.

Acknowledgments

References

1. **Drucker DJ.** The biology of incretin hormones. *Cell Metab*. 2006; 3(3):153–165.

2. **Flint A, Raben A, Astrup A, Holst JJ.** Glucagon-like peptide 1 promotes satiety and suppresses energy intake in humans. *J Clin Invest.* 1998;101(3):515–520.

3. **Verdich C, Flint A, Gutzwiller JP, et al.** A meta-analysis of the effect of glucagon-like peptide-1 (7–36) amide on ad libitum energy intake in humans. *J Clin Endocrinol Metab.* 2001;86(9):4382–4389.

4. **Vilsboll T, Christensen M, Junker AE, Knop FK, Gluud LL.** Effects of glucagon-like peptide-1 receptor agonists on weight loss: systematic review and meta-analyses of randomised controlled trials. *BMJ.* 2012;344:d7771.

5. **Holst JJ.** The physiology of glucagon-like peptide 1. *Physiol Rev.* 2007;87(4):1409–1439.

6. **Campbell JE, Drucker DJ.** Pharmacology, physiology, and mechanisms of incretin hormone action. *Cell Metab.* 2013;17(6):819–837.

7. **Larsen PJ, Tang-Christensen M, Holst JJ, Orskov C.** Distribution of glucagon-like peptide-1 and other preproglucagon-derived peptides in the rat hypothalamus and brainstem. *Neuroscience.* 1997;77(1):257–270.

8. **Blevins JE, Baskin DG.** Hypothalamic-brainstem circuits controlling eating. *Forum Nutr.* 2010;63:133–140.

9. **Shugrue PJ, Lane M, Merchenthaler I.** Glucagon-like peptide-1 receptor (GLP1-R) mRNA in the rat hypothalamus. *Endocrinology.* 1996;137:5159–5162.

10. **Heppner KM, Kirigiti M, Secher A, et al.** Expression and distribution of glucagon-like peptide-1 receptor mRNA, protein and binding in the male nonhuman primate (*Macaca mulatta*) brain. *Endocrinology.* 2015;156(1):255–267.

11. **Williams DL.** Minireview: finding the sweet spot: peripheral versus central glucagon-like peptide 1 action in feeding and glucose homeostasis. *Endocrinology.* 2009;150(7):2997–3001.

12. **Sandoval DA, Bagnol D, Woods SC, D'Alessio DA, Seeley RJ.** Arcuate glucagon-like peptide 1 receptors regulate glucose homeostasis but not food intake. *Diabetes.* 2008;57(8):2046–2054.

13. **McMahon LR, Wellman PJ.** PVN infusion of GLP-1-(7–36) amide suppresses feeding but does not induce aversion or alter locomotion in rats. *Am J Physiol.* 1998;274(1 Pt 2):R23–R29.

14. **Alvarez E, Martinez MD, Roncero I, et al.** The expression of GLP-1 receptor mRNA and protein allows the effect of GLP-1 on glucose metabolism in the human hypothalamus and brainstem. *J Neurochem.* 2005;92(4):798–806.

15. **Alkemade A, Yi CX, Pei L, et al.** AgRP and NPY expression in the human hypothalamic infundibular nucleus correlate with body mass index, whereas changes in αMSH are related to type 2 diabetes. *J Clin Endocrinol Metab.* 2012;97(6):E925–E933.

16. **Kubota K, Ohashi A, Imachi H, Harada H.** Improved in situ hybridization efficiency with locked-nucleic-acid-incorporated DNA probes. *Appl Environ Microbiol.* 2006;72(8):5311–5317.

17. **Siljee JE, Unmehopa UA, Kalsbeek A, Swaab DF, Fliers E, Alkemade A.** Melanocortin 4 receptor distribution in the human hypothalamus. *Eur J Endocrinol.* 2013;168(3):361–369.

18. **Goldstone AP, Unmehopa UA, Bloom SR, Swaab DF.** Hypothalamic NPY and agouti-related protein are increased in human illness but not in Prader-Willi syndrome and other obese subjects. *J Clin Endocrinol Metab.* 2002;87(2):927–937.

19. **Swaab DF, Visser M.** A function for alpha-MSH in fetal development and the presence of an α-MSH-like compound in nervous tissue. *Front Horm Res.* 1977;4:170–178.

20. **Hestiantoro A, Swaab DF.** Changes in estrogen receptor-α and -β in the infundibular nucleus of the human hypothalamus are related to the occurrence of Alzheimer's disease neuropathology. *J Clin Endocrinol Metab.* 2004;89(4):1912–1925.

21. **Borgers AJ, Koopman KE, Bisschop PH, et al.** Decreased serotonin transporter immunoreactivity in the human hypothalamic infundibular nucleus of overweight subjects. *Front Neurosci.* 2014;8:106.

22. **Tang-Christensen M, Vrang N, Larsen PJ.** Glucagon-like peptide 1(7–36) amide's central inhibition of feeding and peripheral inhibition of drinking are abolished by neonatal monosodium glutamate treatment. *Diabetes.* 1998;47(4):530–537.

23. **Xu G, Kaneto H, Laybutt DR, et al.** Downregulation of GLP-1 and GIP receptor expression by hyperglycemia: possible contribution to impaired incretin effects in diabetes. *Diabetes.* 2007;56(6):1551–1558.

24. **Ma X, Bruning J, Ashcroft FM.** Glucagon-like peptide 1 stimulates hypothalamic proopiomelanocortin neurons. *J Neurosci.* 2007;27(27):7125–7129.

25. **Secher A, Jelsing J, Baquero AF, et al.** The arcuate nucleus mediates GLP-1 receptor agonist liraglutide-dependent weight loss. *J Clin Invest.* 2014;124(10):4473–4488.

26. **Yang Y, Moghadam AA, Cordner ZA, Liang NC, Moran TH.** Long term exendin-4 treatment reduces food intake and body weight and alters expression of brain homeostatic and reward markers. *Endocrinology.* 2014;155(9):3473–3483.

27. **van der Stouwe JG, Aeschbacher S, Krisai P, et al.** Plasma levels of glucagon-like peptide 1 and markers of obesity among young and healthy adults. *Clin Endocrinol (Oxf).* 2015;83(5):636–642.

28. **Maida A, Lamont BJ, Cao X, Drucker DJ.** Metformin regulates the incretin receptor axis via a pathway dependent on peroxisome proliferator-activated receptor-α in mice. *Diabetologia.* 2011;54(2):339–349.